Physics of Fluids

# A CFD analysis of gas leaks and aerosol transport in laparoscopic surgery

Cite as: Phys. Fluids **34**, 081905 (2022); https://doi.org/10.1063/5.0097401
Submitted: 28 April 2022 • Accepted: 20 July 2022 • Accepted Manuscript Online: 20 July 2022 •
Published Online: 10 August 2022

Caroline Crowley, Ronan Cahill and Kevin Nolan

Physics of Fluids ARTICLE scitation.org/journal/phf

# A CFD analysis of gas leaks and aerosol transport in laparoscopic surgery

Cite as: Phys. Fluids **34**, 081905 (2022); doi: 10.1063/5.0097401
Submitted: 28 April 2022 · Accepted: 20 July 2022 ·
Published Online: 10 August 2022



Caroline Crowley,[1] Ronan Cahill,[2,3] and Kevin Nolan[1,a)]

## AFFILIATIONS

[1]School of Mechanical and Materials Engineering, University College Dublin, Dublin 4, Ireland
[2]Centre for Precision Surgery, Section of Surgery and Surgical Specialities, School of Medicine, University College Dublin, Dublin 4, Ireland
[3]Department of Surgery, Mater Misericordiae University Hospital, 47 Eccles Street, Dublin 7, Ireland

**Note:** This paper is part of the special topic, Flow and the Virus.
[a)]**Author to whom correspondence should be addressed:** kevin.nolan@ucd.ie

## ABSTRACT

Gas used to distend the abdomen during laparoscopic surgery is released to the external environment when trocar internal valves are opened during instrumentation. Particulate matter, including smoke pollutants and both biological and microbial materials, may be transported within the leakage gas. Here, we quantify the percentage of particulate matter that escape to the airspace and put surgical staff at risk of inhalation using a high-fidelity computational fluid dynamics model, validated with direct Schlieren observation of surgery on a porcine cadaver, to model the gas leak occurring due to the opening of 12 mm trocar valves around insertion/extraction of a 5 mm laparoscopic instrument. Fluid flow was modeled through the internal double-valved geometry of the trocar to a large external region representing the operating room (OR) space. Aerosol particles in the range 0.3–10 $\mu$m were injected into the simulation. A range of intra-abdominal pressures (IAPs) and leakage durations were studied. For gas leak durations of 0.5–1 s, at least 65% of particles reach the surgical team's breathing zone across all IAPs. A typical leak had an estimated volume of 0.476 l of $CO_2$ meaning for a typical laparoscopic operation (averaging 51 instrument exchanges), and 24.3 l escapes via this mechanism alone. Trocar gas-leak emissions propel considerable gas and particle volumes into the OR. Reducing the IAP does not mitigate their long-range travel. This work indicates the potential for powerful computational tools like large eddy simulation to play an impactful role in the design of medical devices such as surgical trocars where complex gas dynamics occur.



## I. INTRODUCTION

The release of pneumoperitoneal gas, used to create intracorporeal working space, during laparoscopic surgery can transport cautery smoke pollutants and potentially infectious matter to the external surgical environment. This hitherto-overlooked issue became a topic of much concern in the healthcare community during the COVID-19 pandemic, due to potential for infectious aerosols through these gas leaks.[1] This led to recommendations not to utilize laparoscopic access early in the pandemic despite its many advantages for patients in general.[2] There is also increasing concern regarding the escape of surgical smoke generated in laparoscopic surgery through the use of heat-producing tools to dissect human tissue. This smoke consists of approximately 5% particulate matter, including chemicals, blood, tissue, bacteria, and viruses.[3] Despite the common presence of positive pressure room ventilation, crowding of the operating table with personnel and equipment creates relative stagnation in the airspace shared by members of the operating room (OR) team.[4]

Instruments in laparoscopic surgery are inserted into the abdomen via valved access trocars, which enable operating without loss of working space achieved by gas (typically carbon dioxide, $CO_2$) distension provided by continuous, pressure-triggered insufflation. Typically, between three and five trocars are used, enabling a surgeon and assistants to operate effectively. A major component of gas emissions occurs though leaks from these trocars, caused by intermittent opening of their internal valves by instrumentation. Figure 1 (Multimedia view) shows a typical arrangement for laparoscopic surgery. Trocars are visible at the bottom of Fig. 1(a), and a plume of laser illuminated smoke is apparent. In Fig. 1(b), Schlieren is used to reveal the structure of the turbulent jet escaping around a surgical instrument inserted into a trocar.

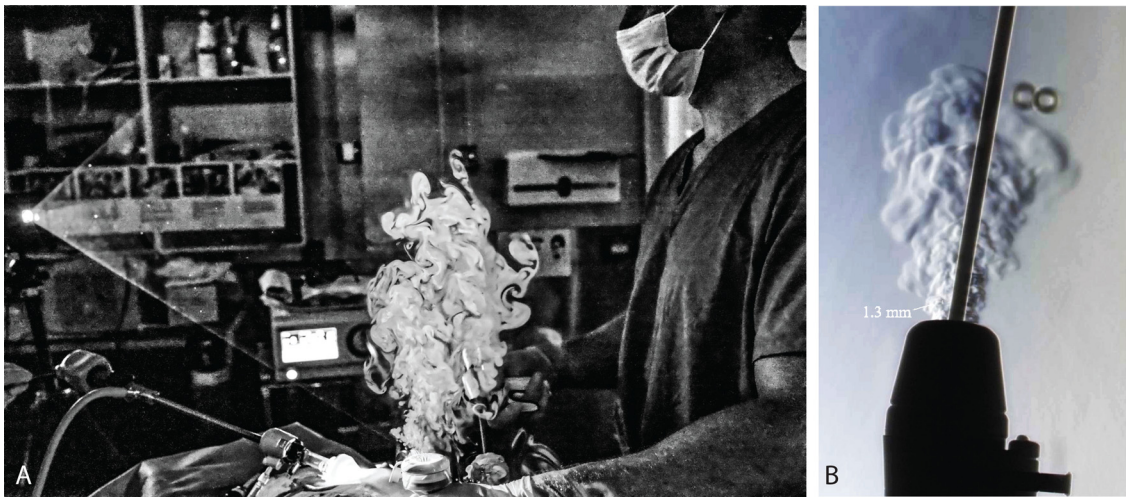


**FIG. 1.** Photographs of leakage during simulated surgery on a porcine cadaver, (a) illuminated by a laser sheet and (B) Schleiren showing detail of the resulting turbulent jet and characteristic length scale. Multimedia view: https://doi.org/10.1063/5.0097401.1

Numerous experimental and observational studies have documented the presence of these leaks. Laser illumination using nebulizers reveals large amounts of smoke released during laparoscopic surgery,[4] while schlieren imaging further confirms their high jet velocity and turbulent nature.[5] Furthermore, it has been shown that the concentration of small particles (0.3–10 $\mu$m) in the OR team breathing zone increases significantly during minimally invasive surgical operations, particularly during the electrocautery dissection,[4] as smoke evacuation systems are often inadequate at removing these smaller particles.[6] However, direct calculation of pollution at both trocar orifice and, especially, surgical team breathing zone level is difficult, given limitations of the sterile surgical field.

To aid understanding of gaseous and particle transport during surgical gas leaks, a numerical model has been developed in this study based on the direct qualitative and quantitative data (both Schlieren revelation of gas leaks and direct particle counting) previously gathered in experimental and observational studies. The primary purpose of the model is to estimate the percentage of particulate matter that may be expelled into the operating airspace of surgeons during a single gas leak due to valve opening with instrumentation under different operating conditions commonly used in surgical practice.

Computational Fluid Dynamics (CFD) has received particular interest in predicting the transport of respiratory particles in fluid flows since the impact of COVID-19. The bulk of the studies on particles–air interactions during breathing, coughing, and sneezing have utilized the Reynolds Average Navier–Stokes (RANS) approach,[7–10] which, although useful in approximating jet characteristics, have notable limitations in accurately resolving the flow field and, therefore, the chaotic trajectory of aerosols due to interaction with inertial turbulent length scales. Large Eddy Simulation (LES) allows these larger turbulent flow structures to be resolved, hence providing a much closer representation of reality, and have been utilized with a high degree of success in modeling particles transport in indoor environments.[11–14]

## II. MODEL DESCRIPTION

### A. Model overview

The CFD model represents a gas leak occurring from a standard trocar due to the failure of the internal valves, modeled here as a small rigid opening, caused by surgical instrument insertion. While there are different brands of trocar made by different manufacturers, a typical trocar has two internal valves: a lower cross slit valve and an upper diaphragm valve. While different trocar sizes are used, commonly used trocars have either a 5 or 12 mm internal diameter. Through these, instruments of different diameters are placed ranging from a camera for observation to graspers to hold tissue, and cutters and energy devices to dissect tissue and ensure hemostasis. Previous work has documented gas leak emission flow rates, using both Schlieren imaging and mechanical test equipment, during the insertion of different instruments in different trocars at different intra-abdominal gas pressures (IAPs).[5,15] In addition, both we and others have measured particle counts and sizes at trocar level during surgery.[4] While 12 mm Hg (1.6 kPa) is the standard operating pressure used in general surgery, low pressure operating (8 mm Hg) is increasingly advocated[16] (assuming sufficient visualization can be achieved) and high pressure (20–25 mm Hg) is sometimes used especially in urological and gynaecological operations to help with bleeding control and offset pressure loss during certain procedures.

### B. Governing equations

Two sets of governing equations were required to model the two-phase flow. First, the time-dependent Navier–Stokes equations for mass [Eq. (1)] and momentum [Eq. (2)] were employed to describe the continuous phase (i.e., the gas leak and surrounding air),

$$\frac{\partial \rho}{\partial t} + \nabla \cdot (\rho \vec{v}) = S_m, \tag{1}$$

$$\frac{\partial}{\partial t}(\rho \vec{v}) + \nabla \cdot (\rho \vec{v}\,\vec{v}) = -\nabla p + \nabla \cdot \tau + \rho \vec{g} + \vec{F}, \tag{2}$$

where $S_m$ is a source term for the addition of mass from a dispersed phase.

The Navier–Stokes equations are filtered for LES, based on the eddy whose scales are less than the grid spacing employed in the computation mesh. The dynamics of larger eddies are, therefore, fully resolved, while time-averaged values are calculated for sub-grid structures. The Wall-Adapting Local Eddy-Viscosity (WALE) model is employed herein[17] due to its robustness and a lower computational demand for flows in complex geometries and with unstructured grids compared to the standard and filtered Smagorinsky models. Recent studies (e.g., Calmet *et al.*[14] and Akagi *et al.*[18]) in which particle-laden flow travels through complex internal pathways to external surroundings report a high degree of success.

Second, the Lagrangian Particle Tracking (LPT) method was used to calculate the position and velocity $\vec{u}_p$ of the discrete phase (particles) in the fluid phase with velocity $\vec{u}$. The force balance is given by

$$\frac{d\vec{u}_p}{dt} = F_D(\vec{u} - \vec{u}_p) + \frac{\vec{g}(\rho_p - rho)}{\rho_p} + \vec{F}, \tag{3}$$

where $\vec{F}$ is an additional acceleration term due to forces including virtual mass, buoyancy force, pressure force, and Magnus force. The drag force is

$$F_D = \frac{18\mu}{\rho_p d_p^2}\frac{C_D Re}{24}. \tag{4}$$

Here, the particles are assumed to be spheres of constant volume ($\pi d_p^3/6$), with no phase change taking place. The particle density $\rho_p$ is assumed to be much greater than that of the surrounding fluid, meaning drag force $F_D$ is considerably larger than other forces that may be acting on the particle, and therefore, $\vec{F}$ may be neglected.[19]

### C. Geometry

A 3D computer aided design (CAD) model, designed in ANSYS CAD modeling software SpaceClaim, was developed consisting of a 12 mm trocar and a generic 5 mm diameter instrument, as shown in Fig. 2. The lower valve is a cross-slit valved modeled in an "open" position, and the upper diaphragm valve is modeled with a 2 mm clearance from the instrument. A 40 mm section of cannula is also included. The computational domain consists of the internal fluid in the trocar and a cylindrical external region of 500 mm height and 240 mm diameter (see Fig. 3), a volume equating to that shared by the OR team above the patient. The computational mesh was generated using the ANSYS Fluent meshing utility. The mesh contains $5.3 \times 10^6$ elements, made up predominantly of tetrahedral cells. Regions of refinement were added in the internal fluid area and the external region at the trocar outlet. The smallest cell size (0.60 mm) was calculated based on half the size of the smallest eddies as measured from schlieren images extracted from video footage recorded at 8K resolution. Ten inflation layers are applied to the walls of the trocar, made up of hexahedral cells.

### D. Solution method

Large Eddie Simulation (LES) was used to simulate the $CO_2$ jet. Herein, the larger scale energy-carrying eddies, clearly visible in the experimental recordings of the turbulent jets released during the gas leaks, are fully resolved, while the smaller energy-dissipating eddies are numerically modeled. As mentioned above, the Wall-Adapting Local-Eddy Viscosity (WALE) model[17] was used to perform the transient simulations in ANSYS Fluent 2021R1. A time step of 0.0001 s was used, allowing a Courant number $\leq 1$.

Discretization in space was achieved using the least squares cell based method. The second order scheme was used for pressure and $CO_2$ terms, and the bounded central differencing scheme for momentum. A bounded second order implicit scheme was used for time discretization to ensure stability of the solution. The coupled algorithm was employed for pressure–velocity coupling. A maximum of 50 iterations were allowed per time step, and no specific convergence criteria were given.

### E. Boundary conditions and physical model

The base of the cannula was defined as a pressure inlet. Both inlet pressure and duration were varied as outlined in Table I. A no-slip

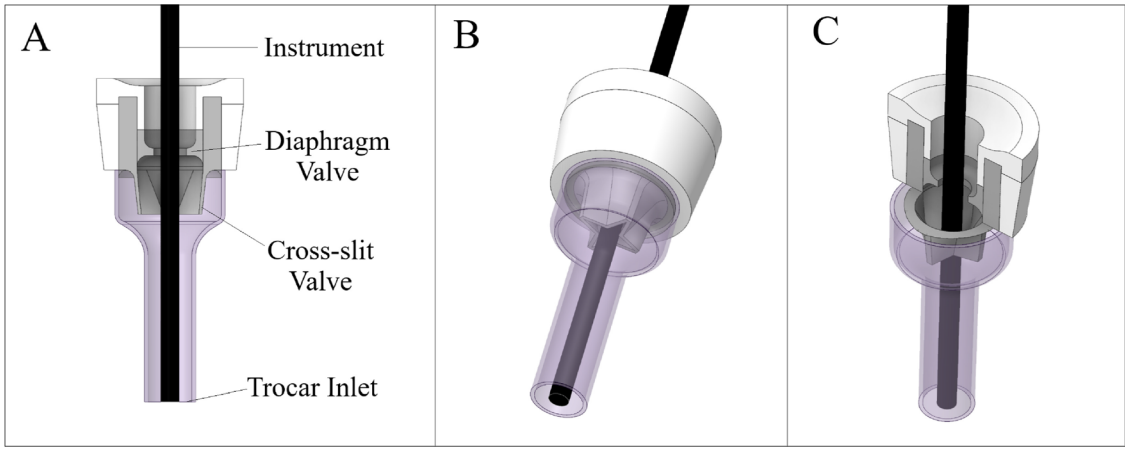


**FIG. 2.** CAD model of the trocar with instrument inserted used in the CFD simulation showing different perspectives of the internal structure of the valves (a)–(c).

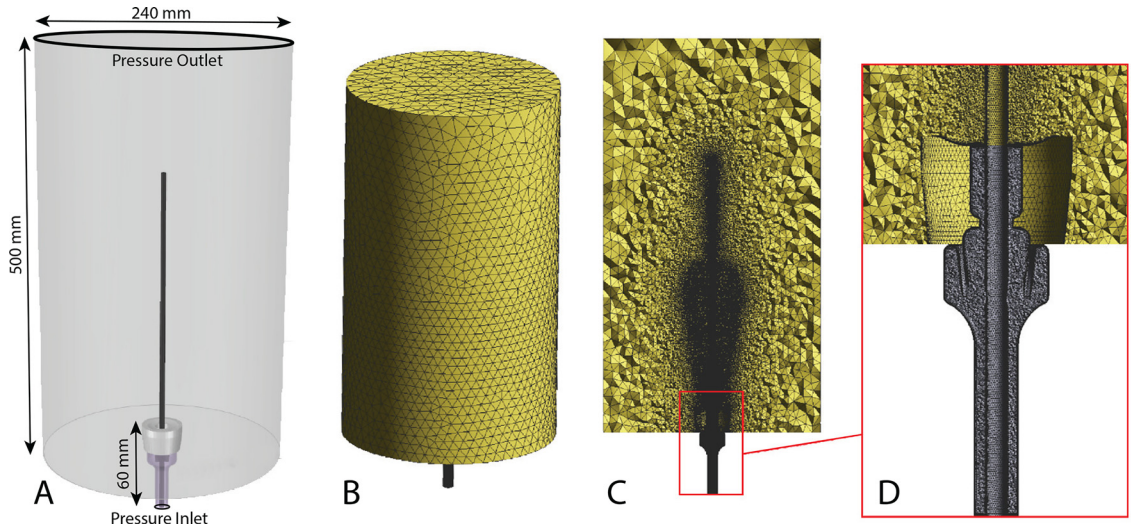


**FIG. 3.** Schematic of fluid domain (a) indicating overall dimensions and boundary conditions. (b) Entire mesh geometry showing the external cylindrical region of fluid representative of section of OR space. (c) Section view through the mesh showing regions of refinement with (d) a magnified image of the internal trocar fluid region.

condition was applied to the trocar and instrument walls, and the external cylinder walls were open to the atmosphere. The upper cylinder face was set as a pressure outlet and the outer cylinder walls set to a zero-flux condition. Particles were reflected from the trocar walls and inlet but allowed to escape through the pressure outlet.

A two-phase flow is modeled in which the bulk fluid (continuous phase) follows the Eulerian approach and the particles (discrete phase) follow the Lagrangian approach. The continuous phase was initially stagnant air at zero-gauge pressure and was modeled as incompressible flow. $CO_2$, which is used for insufflation of the abdomen, was released from the pressure inlet at the start of the simulation, hence leading to a mixture of gases in the continuous phase. The gases are non-reacting with respect to both each other and the released particles.

The discrete phase consists of the particles that were injected at the trocar inlet, and their paths tracked for the duration of the simulation. Particles were modeled as water particles—a reasonable assumption, given surgical smoke comprises 95% water and 5% particulate matter.[3] The size distribution of the particles injected was based on those recorded during a variety of elective laparoscopic surgeries.[4] A single injection consisted of equal populations of particles with fixed diameters of 0.3, 0.5, 1, 2.5, 5, and 10 $\mu$m. The particles were injected across a plane at the trocar inlet [see Fig. 2(a)]. A single particle of each size was released from each cell face at the pressure inlet (647 faces in total) corresponding to a total of 3884 particles per injection. A total of three injections were implemented at time steps of 0, 0.05, and 0.1 s. The bulk flow influenced the particle trajectories, but the particles had no effect on the bulk fluid, i.e., one way coupling. This was a reasonable assumption due to the minute size and number of the particles introduced. The non-reacting particles were tracked through the flow for 3 s after release. All simulated cases followed the same particle injection setup.

**TABLE I.** Summary of simulated cases.

| Case | IAP | Leakage duration | Particle range |
|---|---|---|---|
| Standard pressure, standard duration | 12 mm Hg | 0.5 s | 0.3–10 $\mu$m |
| Low pressure, standard duration | 8 mm Hg | 0.5 s | 0.3–10 $\mu$m |
| High pressure, standard duration | 15 mm Hg | 0.5 s | 0.3–10 $\mu$m |
| Very high pressure, standard duration | 20 mm Hg | 0.5 s | 0.3–10 $\mu$m |
| Standard pressure, short duration | 12 mm Hg | 0.13 s | 0.3–10 $\mu$m |
| Standard pressure, long duration | 12 mm Hg | 1.0 s | 0.3–10 $\mu$m |

### F. Simulated cases

The 12 mm trocar–5 mm instrument configuration was the sole configuration investigated as this was taken to be the worst case scenario. A 5 mm trocar matched with a 5 mm instrument configuration has been proven to be associated with lower leakage flow rates. Higher leakage flow rates have been observed with the insertion of an obturator into 5 mm trocars.[5,15] However, the extremely narrow clearance with the trocar cannula makes the configuration unsuited for CFD analysis without further characterization of the geometry.

The model was validated and used to investigate different leakage scenarios. The standard case was defined as a 12 mm Hg IAP with a 0.5 s leak duration, as timed from schlieren imaging recordings. Three alternative IAP settings were simulated, 8, 15, and 20 mm Hg, accounting for low and high pneumoperitoneal pressures used in laparoscopic surgery. Additionally, two alternative leakage durations were

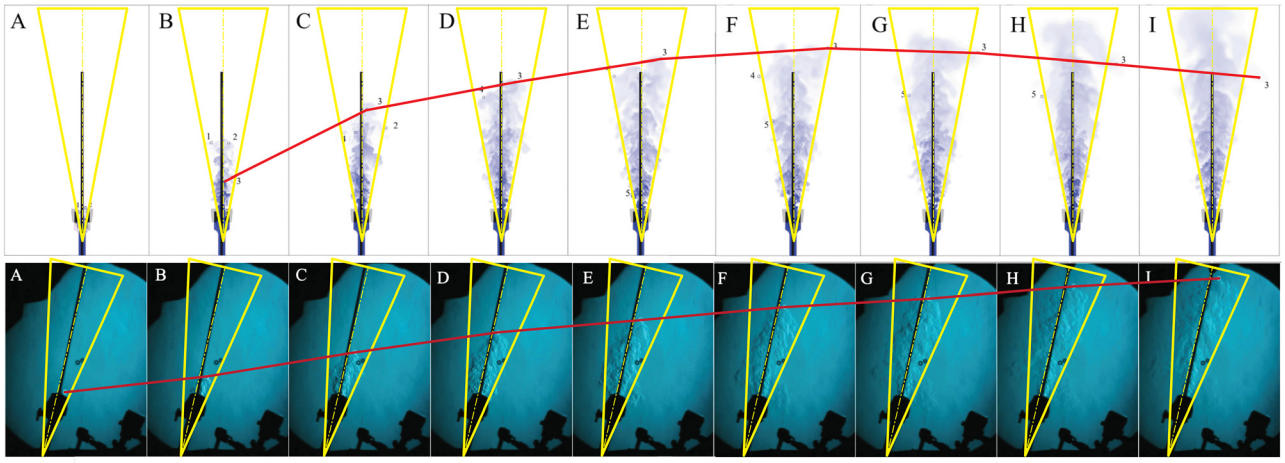


**FIG. 4.** Image sequences (a)–(i) for (top) simulation $CO_2$ mass fraction and (bottom) Schlieren visualization of a trocar leak around a surgical instrument. The time sequence corresponds to time step of 30 Hz. Each frame is connected via by a (red) line showing the advection of a coherent structure tracked between frames. An isosceles triangle (yellow) with a spread angle of 22° is copied to each frame. The vertical field of view for the simulation is 0.5 m, and for the Schlieren 0.4 m, the field of view of the mirror.

simulated, 0.13 and 1.0 s, accounting for short and long duration leaks, respectively. Full details of the simulated cases are outlined in Table I.

## III. RESULTS

### A. Model validation

Schlieren typically provides qualitative data in the form of flow visualization in comparison to more sophisticated techniques such as particle image velocimetry typically used for quantitative validation of CFD. However, it is not practical to deploy a Particle Image Velocimetry (PIV) facility in a surgical theater. Quantitative validation of the present results may, however, be achieved in a number of ways: tracking of the advection of discrete flow structures, direct measurement of the jet spreading angle, and time-space slices of the turbulent flow field. A summary of the former two methods is shown in Fig. 4. It is observed that the spreading angle is consistent within a 22° envelope. Figure 5 plots the velocity of several tracked structures compared to those observed in Schlieren. While tracked points tend to have a large initial velocity, the data converge to match the Schlieren. This indicates that the configuration of the valve in the simulation does not fully represent that of a trocar.

Time–space plots were constructed by taking slices through the video data at a single column of pixels, specific feature tracking and spreading angle measurement, Fig. 6. A slice of pixels is extracted for a sequence of video frames and a time-space plot constructed. The slope of coherent features in the time-space plot represents the velocity of flow structures in the jet. The same process is performed for the simulation data. Lines of equal slope are shown in Fig. 6, further indicating that the simulation captures the dynamics of the experimental data.

Discrepancies may be explained by observing that numerical flow fields were taken in the center plane of the jet, while the schlieren footage integrates across the volume of the jet, including the boundary where the velocity is lower. Figure 7 (Multimedia view) shows a comparison between experimentally obtained schlieren images of typical gas leaks occurring with 5 mm instruments in 12 mm trocars at 12 mm Hg IAP and the standard case simulated by the CFD model. The volume of $CO_2$ released in the CFD simulation [Fig. 7(b)] can be seen to closely resemble the shape of the gas jet captured in the schlieren image [Fig. 7(a)] with similar spreading angles observed. Figure 7(c) shows the light sheet obtained using a laser light sheet illuminating a 2D slice of the airspace above a porcine cadaver undergoing surgery, and Fig. 7(d) shows a contour plot of the $CO_2$ mass fraction in a plane through the center of the trocar. Due to the fine mesh used in the model, the structure of the small eddies is captured in the CFD model, meaning the influence of turbulence in the jet on the particle trajectories is accounted for.

### B. Internal flow

Figure 8 shows the velocity distribution in the mid-plane of the internal trocar region for each of the four pressure settings simulated.

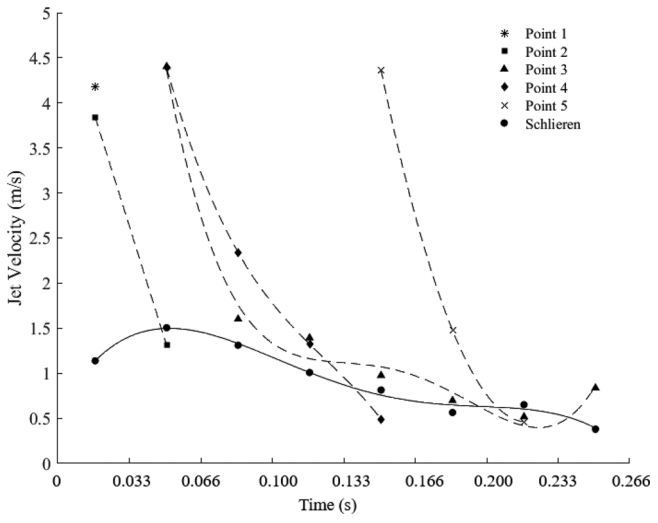


**FIG. 5.** Structure velocity at the specific points tracked in the CFD model (dashed lines) and 30 FPS schlieren (continuous line) over the initial time steps.

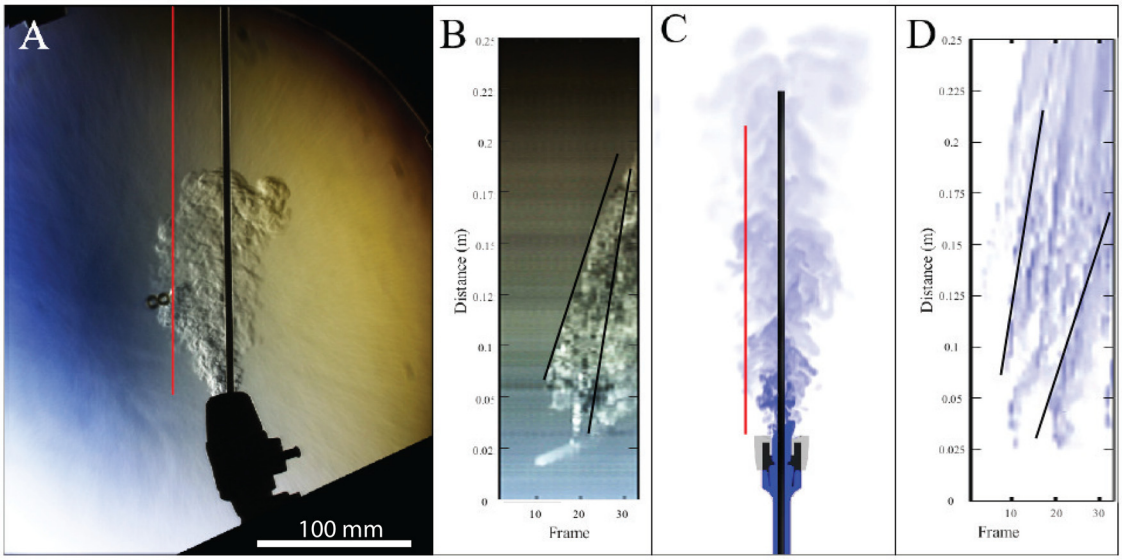


**FIG. 6.** Validation of numerical simulation, for IAP = 12 mm Hg and leakage duration = 0.5 s and 5 mm diameter instrument, showing (a) location of time-space slice in Schlieren data, (b) resulting time-space plot, (c) simulated jet, and (d) numerical time-space plot. Lines of equal slope are shown on both time-space plots.

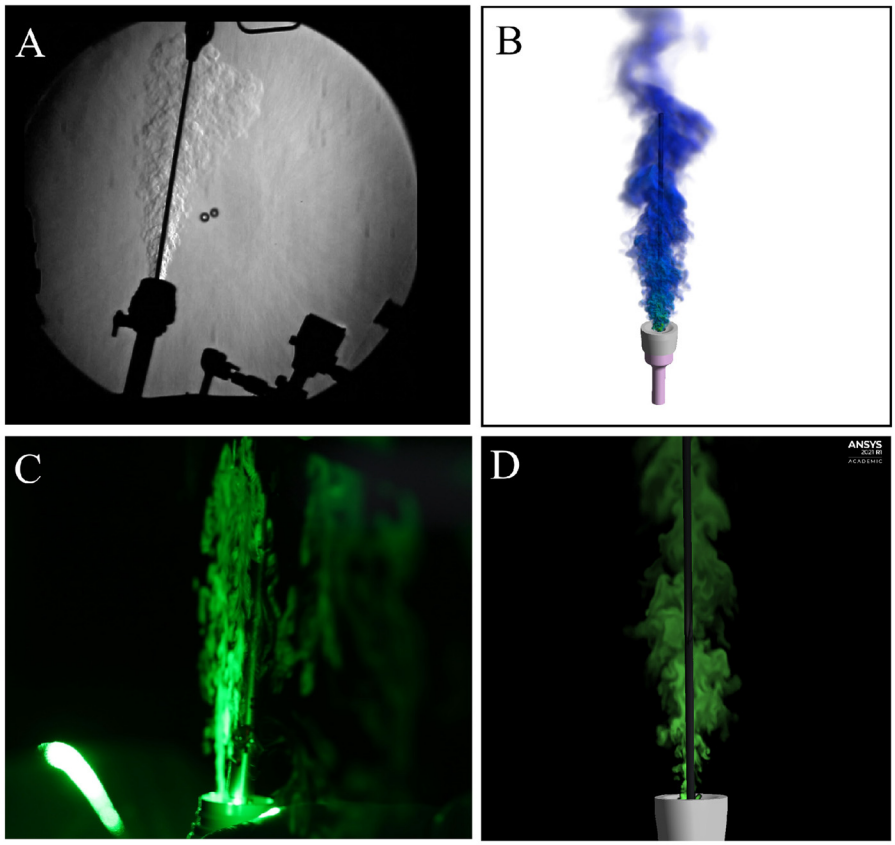


**FIG. 7.** (a) Schlieren image of a gas leak from a 12 mm trocar at an intra-abdominal pressure of 12 mm Hg. (b) Volume rendering of the standard case CFD simulation showing $CO_2$ volume released in a gas leak. (C) Visualization of a gas leakage from a 12 mm trocar due to camera insertion using an illuminating laser sheet. (D) Contour plot of $CO_2$ mass fraction across a plane through the center of the trocar. Multimedia view: https://doi.org/10.1063/5.0097401.2

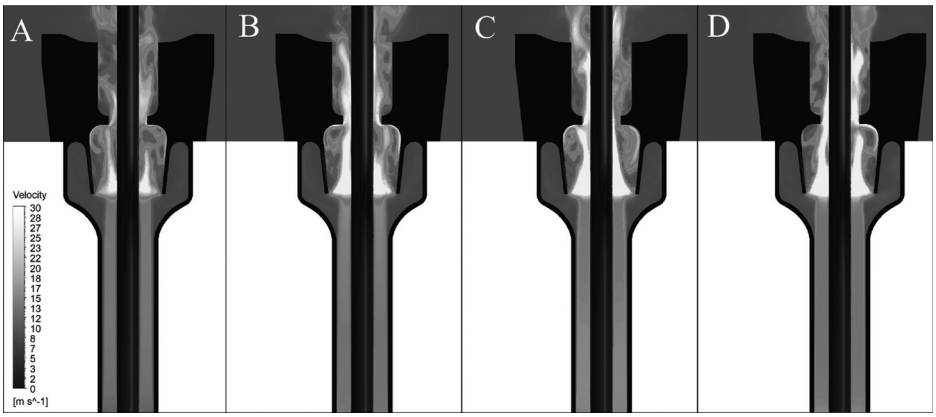


**FIG. 8.** Instantaneous velocity profiles in the internal trocar region at t = 0.5 s for intra-abdominal pressures of (a) 8 mm Hg, (b) 12 mm Hg, (c) 15 mm Hg, and (d) 20 mm Hg.

The velocity increases to a maximum at the point where the flow enters the reduced area of the cross-slit valve corresponding to a "leak" state. Note that since the valves are modeled as a rigid structure in a partially open configuration, the increase in IAP does not influence their shape here. The current work is intended to understand the leaks that are observed to occur experimentally and in clinical settings during instrument changes. Initial trials carried out with only this lower valve showed a higher velocity at the outlet—i.e., the second, upper valve slowed down the flow. Experimental observations show that leaks occur even with both valves in place. The velocity magnitude increases with increasing IAP, reaching over 30 m/s in a large portion of the inner trocar for the 20 mm Hg case. The generation of turbulence is observed between the valves and the outlet of the trocar in all cases.

### C. Leakage flow rate and $CO_2$ volume released

The total volume of $CO_2$ released in a single leak was estimated by obtaining the volume flow rate at the trocar outlet during the leakage and multiplying this by the leakage duration. The results are outlined in Table II. An increasing intra-abdominal pressure was associated with an increasing flow rate and, hence, increasing total volume of gas released. An increased duration was also associated with a larger amount of gas released.

### D. Particle dispersion

The positions of the particles released at the inlet were tracked throughout the simulation to determine how the $CO_2$ jet transports material through the trocar into the airspace above a patient. The final positions of the particles were grouped into three different categories: (i) trapped inside the trocar; (ii) in the vicinity of the trocar (within 0.5 m of the trocar outlet); and (iii) escaped to the surgeons airspace (beyond 0.5 m from trocar outlet).

**TABLE II.** Flow rate and calculated volume of $CO_2$ released.

| IAP and duration | Flow rate at trocar outlet | $CO_2$ released |
|---|---|---|
| 8 mm Hg, 0.5 s | 46.08 l/min | 0.384 l |
| 12 mm Hg, 0.5 s | 57.14 l/min | 0.476 l |
| 15 mm Hg, 0.5 s | 63.82 l/min | 0.532 l |
| 20 mm Hg, 0.5 s | 76.12 l/min | 0.634 l |
| 12 mm Hg, 0.13 s | 57.13 l/min | 0.124 l |
| 12 mm Hg, 1.0 s | 59.05 l/min | 0.984 l |

The final positions were taken at the final time step of the simulation, i.e., t = 3 s. This was considered reasonable as comparison between the particle numbers in each category showed little variation between t = 2 s and t = 3 s. The results as outlined in Fig. 9 give the total particle number in each category as a percentage of the total number of particles injected. This includes all injections and all particle diameters. In all cases, the largest percentage of particles were located beyond 0.5 m of the trocar vertically or within the surgeons airspace. This varied between 58.12% for the short duration, standard pressure case and 84.34% for the very high pressure case. A very small amount of particles remained trapped in the trocar, typically below 1%. This was notably higher for the short duration case at 7.56%. The remaining particles were located within the vicinity of the trocar (14.97%–34.32%), see Fig. 7.

## DISCUSSION

Laparoscopic surgery is the procedure of choice for many elective surgical operations, due to reduced patient morbidity, increased patient comfort, and shorter recovery times. While evidence to support the claims that COVID-19 can be transmitted in this manner is mixed,[20–22] the confirmation of Human papillomavirus (HPV) transmission through minimally invasive surgery[16] indicates that the potential for transmission of existing and, indeed, any new virus is a non-negligible risk. While laparoscopic operating has generally been resumed, as it stands, the risk of infectious transmission remains, and coupled with the large amounts of pollutant-laden smoke released to the external surgical environment, it is clear that the safety of OR staff is compromised in these routine procedures (and also that further disruptions to standard surgical procedures are likely to arise in future cases of new viral pandemics). However, the problem of gas leaks and associated surgical smoke contamination within the OR can be difficult to detect and consequently often ignored. It is, therefore, essential that not only best practices are followed, but also rigorous scientific methodology is applied to fully understand the issues as much supposition and opinion currently exist. Better characterization of the

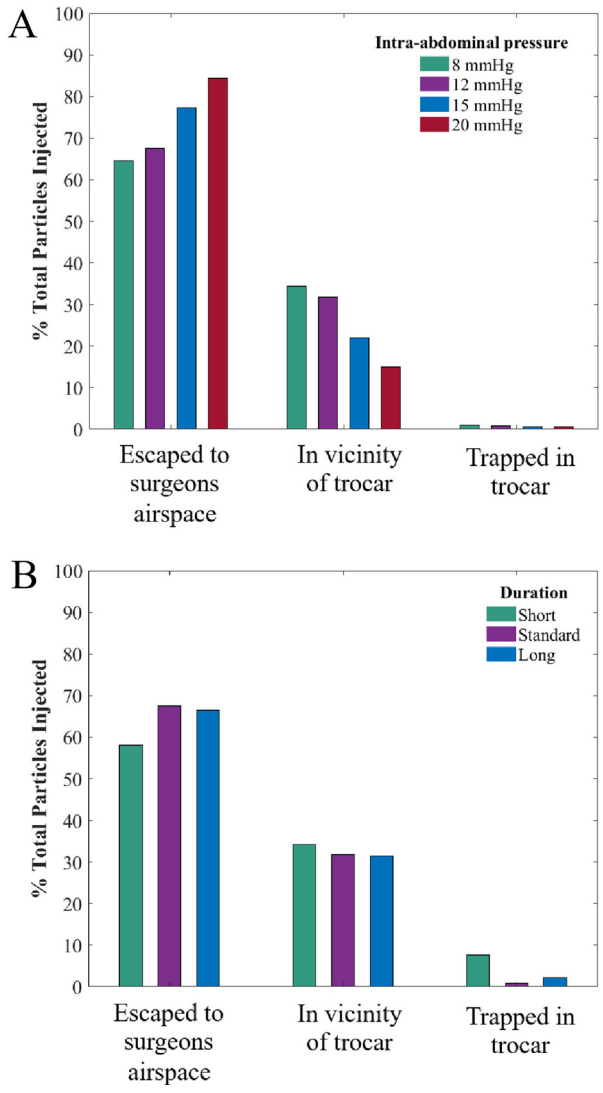


**FIG. 9.** Final particle positions (at t = 3 s) for different (a) IAPs and (b) leakage durations. Particle quantity is given as a percentage of the total number of particles released in all injections.

problem areas will lead to better understanding and, where needed, optimization of surgical instruments and practice.

This study provides novel information about the flow dynamics of gas leaks from trocars during laparoscopic surgery and the trajectories of particles ejected in the leaks, using a high-fidelity CFD simulation. While other mechanisms of gas leaks exist, those occurring via trocar valves are in built into the trocar design and are, therefore, not controllable by changes in surgeon behavior or practice. While particle counts and gas leaks can be directly measured at source, it is much harder to extrapolate to the level of the OR breathing zone due to the specifics of OR rooms, which require respect of sterile field and no distraction to the surgical team focused on performing invasive intervention safely. Experimental validation of the simulation showed that the model captures the dynamics of the leaks with an acceptable degree of accuracy given the simplifications of the trocar geometry.

Based on the median number of instrument changes in a typical laparoscopic surgery of 51,[23] a total volume of 24.3 l of $CO_2$ is estimated to be released when a standard intra-abdominal pressure of 12 mm Hg is used, and a single leak occurs at each instrument exchange. Although using a lower pressure setting of 8 mm Hg results in a lower outlet flow rate and, hence, a smaller volume of $CO_2$ being released of 19.6 l, the gas release is still clearly not negligible. Furthermore, 65% of the particles ejected in the gas release reach the surgeons airspace for the "low" pressure setting. This is barely distinguishable from the 68% of particles reaching this region for the standard pressure setting. On the other hand, the "very high" pressure setting results in an estimated $CO_2$ volume of 32.3 l released, and 84% of particles escape to the surgeons airspace. While it has been generally advised that pneumoperitoneum should be maintained at the lowest possible pressure,[16] the simulation results show that use of low pressure does not fully alleviate the problem (although clearly high pressures should be avoided). Extra precautions should undoubtedly be taken to protect OR staff from pollutants and particles carried in the gas leaks.

A key aspect of this study, alongside its direct grounding in directly observed imagery obtained experimentally during cadaveric surgery, is the implementation of representative particles in the CFD model of the size, which may carry bacteria, viruses, hazardous chemicals, and human tissues.[3] The range of particle sizes used has been experimentally shown to be emitted in laparoscopic surgery in large quantities.[4] Quantifying the exact number of particles emitted in a single leak is difficult due to large variability, and so this study can only provide an indicator of the fraction that is transferred to a region that puts OR staff at risk. Larger particles were neglected in this study, as these typically follow a ballistic trajectory governed by the influence of gravity and drag forces, while smaller particles remain entrained in high-velocity flow fields.[24,25] Since these small particles have very low settling velocities, they are likely to remain airborne in the vicinity of the surgeons for extended periods of time.[26] Additionally, surgical face masks provide a good level of protection from larger particles, showing a 25 fold reduction in penetration counts for particles above 5 $\mu$m. On the other hand, surgical masks only reduce penetration counts for particles below 5 $\mu$m by 2.8 fold.[27]

Importantly, particles of 10 $\mu$m or less can be inhaled by surgeons, with those less than 2.5 $\mu$m reaching the lower airways.[4] Nanoparticles, of slightly below the investigated particle size ($<0.1$ $\mu$m), are the main source of danger of inhaled smoke, causing an increased risk of disease, such as Parkinsons, Alzheimer's, and various cancers through chronic exposure.[28] Taking into account the general preference to wear surgical masks over more effective, but notably less comfortable, respiratory masks as well as leakage issues associated with ill-fitting masks,[29] it is clear that personal protective equipment (PPE) alone is not enough to fully protect OR staff from the aerosolized particles emitted in gas leaks.

One of the main limitations of this study is the idealization of the gas leak investigated. Schlieren images show large variation in the position of the jet and angle at which gas leaks occur. This is primarily due to different locations of failure of the valves based on the angle at which the instrument is inserted/extracted during surgery. In this study, a perfectly symmetrical failure is modeled in the simulation,

with the instrument inserted vertically and all sides of the valves having equal clearance from the instrument. Additionally, the geometry of the model is static and rigid throughout the simulation. Although a stationary instrument inside a trocar port has been shown to still produce a gas leak,[30] in real-life surgical scenarios, the instrument is almost constantly moving against the valve as it is inserted/extracted, causing the shape of the valve and area of leakage to change in response. Due to this interaction, the gas leaks are generally intermittent in nature, while in the simulated cases, all leaks were single, continuous pressure releases. Additionally, the positions of the valves were identical for all IAPs applied. In reality, a higher pressure setting is likely to affect the conformation of the valve around the instrument, making it more tightly fitted to the instrument. Capturing the dynamic nature of the leakage due to interaction between instruments, trocar valves and different IAPs would require further experimental observations and implementation of a coupled fluid–structure interaction (FSI) model.

Additionally, the flow rates recorded at the trocar outlet ranged between 46 l/min for the 8 mm Hg pressure setting and 76 l/min for 20 mm Hg. This is higher than the maximum flow rates estimated in our previous experimental studies of 20 l/min.[5] However, these values were estimated using the optical flow method, which underestimates the flow rates as we track vortices shed by the jet. Additionally, these were indicative volumetric flow rates associated with instruments matched to the internal diameter of the trocar channels. The estimated total gas released per instrument exchange of between 0.384 and 0.634 l is also notably higher than the 0.029 47–0.041 32 l estimated from experimental studies with the same trocar/instrument configuration.[30] The compromised configuration of both valves in the present work where a significant gap is present accounts for much of this discrepancy. Experimental studies in this area are limited, and the mechanisms of valve failure are not documented. It may be hypothesized that the dual valves act to gate escaping gas as the volume between valves becomes pressured at instrument insertion and then released upon instrument removal limiting escaping volume. This, however, does not account for the leaks observed on instrument insertion where the diaphragm valve does not prevent leakage.

Furthermore, validation of the simulation confirmed the jet velocities to be in the range 4–4.5 m/s in the region near the trocar outlet, which is in agreement with maximum jet velocities of 5 m/s reported.[5] This decayed to 0.5–1 m/s in the outer region, which matches the values estimated from tracking of schlieren recordings.

A further potential cause of the high flow rates is the continuous pressure applied at the inlet in the model for the given duration. As gas is released through the leakage, it would be expected that internal pressure would drop, thereby also causing a drop in the model inlet pressure. Further developments of the model may see the use of inlet conditions based on an experimentally obtained velocity or pressure profiles taken within the trocar during a leakage.

The average duration of the gas leaks during laparoscopic surgery is difficult to quantify due to the variability in the length of time for which a trocar valve fails. As seen in experimental studies, the leaks can generally be characterized as short-lived, turbulent bursts, or jets of gas. While the median time for a single instrument switch is 0.13 min,[23] the gas leak is typically much shorter than this, usually occurring at the initial penetration of the instrument in the valves (releasing the gas trapped between the two). In this study, durations of 0.13, 0.5, and 1.0 s were investigated to give a range across short timeframes. The particle count reaching the surgeons airspace proved lower for the short duration leak (58%), but no major difference was observed between the intermediate and long duration leaks. In fact, the long duration leak was associated with a very slight decrease in particles in the far-field region. This indicates that IAP has a greater effect on particle dispersion than leak duration in the current computational configuration. It should be noted that in the simulation, the same quantity of particles was ejected for all leak durations simulated. In reality, particles are ejected continuously as opposed to discrete injections, and so we would expect to see a greater quantity of particles released for a long duration leak.

Herein, we consider populations of particles informed by measurements taken in the airspace above patients in live surgery. Particles are reflected from trocar walls and are not, therefore, readily captured in the flow geometry. The intent of this is to observe transport of smoke and other particles in theater; however, the efficient capture of particles within the trocar should represent a design goal for medical device designers. Sophisticated numerical modeling has been used to investigate particle deposition and capture in respiratory tracts[31] and cascade impactors.[32] These approaches suggest a way forward for industry to mitigate the risks associated with their products.

## CONCLUSION

In conclusion, as a computer-simulated study, the results of the investigation should be taken as complementary evidence of gas leaks and associated aerosol dispersion to existing experimental and clinical evidence. The detailed CFD model implemented indicates that over 60% of particulate matter released from within the abdomen during a typical gas leak will reach a region of the surgical theater, in which they are likely to be inhaled by surgical staff. Additionally, 24.3 l of gas may be released to the external surgical environment via this mechanism during a typical elective surgery. The study provides further support for existing recommendations regarding the safety of OR staff during laparoscopic surgeries including minimizing the number of instrument exchanges, quick insertion and removal of surgical instruments, and use of the lowest intra-abdominal pressure possible.[15] Completion of desufflation before trocar removal, use of air purifiers, and adequate room ventilation should also be considered.[16] It should be evident, however, that these precautions will not fully mitigate the risk of gas leaks occurring, and so there is still a need for the development of new technologies and engineering solutions to help mitigate these leaks at the root cause and help make ORs a safe workspace for hospital staff. This may come in the form of improved valve design, to ensure the seal between the trocar and instrument does not fail during surgery and may entail further research into superior valve types and anti-fatigue materials. Other possible solutions may see the implementation of built-in suction technology to determine the jet and encapsulated particles from entering the external environment.

## ACKNOWLEDGMENTS

The authors wish to thank Dr. Malachy O'Rourke (University College Dublin) for his expertise and support in setting up the ANSYS software package. The authors also wish to thank the Mater Misericordiae University Hospital for facilitating experimental work, with particular thanks to the surgical staff for offering assistance and sharing their medical knowledge. The authors wish to acknowledge the Irish Centre for High-End Computing (ICHEC)

and the ResearchIT Sonic cluster (funded by UCD IT Services and the Research Office) for the provision of computational facilities and support. This project has received funding from the European Union's Horizon 2020 research and innovation programme under Grant Agreement No. 101015941 for the PORSAV (Protecting Operating Room Staff Against Viruses) research programme.

## AUTHOR DECLARATIONS

### Conflict of Interest

The authors have no conflicts to disclose.

### Ethical Approval

Ethical approval for this work was granted by the Mater Misericordiae University Hospital Institutional Review Board, Reference No. 1/378/2172, under the AeroSolve study.

### Author Contributions

**Caroline Crowley:** Conceptualization (equal); Data curation (lead); Formal analysis (equal); Methodology (equal); Software (lead); Validation (equal); Visualization (lead); Writing – original draft (lead); Writing – review and editing (equal). **Ronan Cahill:** Conceptualization (supporting); Funding acquisition (lead); Investigation (supporting); Project administration (supporting); Resources (supporting); Supervision (supporting); Writing – original draft (supporting); Writing – review and editing (supporting). **Kevin Patrick Nolan:** Conceptualization (equal); Data curation (supporting); Formal analysis (equal); Funding acquisition (supporting); Investigation (equal); Methodology (supporting); Project administration (lead); Resources (supporting); Software (supporting); Supervision (lead); Validation (supporting); Visualization (supporting); Writing – original draft (equal); Writing – review and editing (lead).

## DATA AVAILABILITY

The data that support the findings of this study are available from the corresponding author upon reasonable request.

## REFERENCES

[1]S. Emile, "Should we continue using laparoscopy amid the COVID-19 pandemic?," Br. J. Surg. **107**, e240 (2020).
[2]Royal College of Surgeons of Edinburgh (RCSEd), Association of Surgeons of Great Britain & Ireland, Association of Coloproctology of Great Britain & Ireland, Association of Upper Gastrointestinal Surgery, Royal College of Surgeons of England, Royal College of Physicians and Surgeons of Glasgow, and Royal College of Surgeons in Ireland, *Updated General Surgery Guidance on COVID-19, 2nd Revision* (Royal College of Surgeons, 2020).
[3]B. C. Ulmer, "The hazards of surgical smoke," AORN J. **87**, 721 (2008).
[4]N. Hardy, J. Dalli, M. Khan, K. Nolan, and R. Cahill, "Aerosols, airflow, and airspace contamination during laparoscopy," Br. J. Surg. **108**(9), 1022–1025 (2021).
[5]R. A. Cahill, J. Dalli, M. Khan, M. Flood, and K. Nolan, "Solving the problems of gas leakage at laparoscopy," Br. J. Surg. **107**, 1401–1405 (2020).
[6]T. de Boorder, R. Verdaasdonk, and J. Klaessens, "The visualization of surgical smoke produced by energy delivery devices: Significance and effectiveness of evacuation systems," Proc. SPIE **6440**, 64400R (2007).
[7]T. Dbouk and D. Drikakis, "On coughing and airborne droplet transmission to humans," Phys. Fluids **32**, 053310 (2020).
[8]T. Dbouk and D. Drikakis, "On respiratory droplets and face masks," Phys. Fluids **32**, 063303 (2020).
[9]Z. Zhang, T. Han, K. H. Yoo, J. Capecelatro, A. L. Boehman, and K. Maki, "Disease transmission through expiratory aerosols on an urban bus," Phys. Fluids **33**, 015116 (2021).
[10]R. Biswas, A. Pal, R. Pal, S. Sarkar, and A. Mukhopadhyay, "Risk assessment of COVID infection by respiratory droplets from cough for various ventilation scenarios inside an elevator: An OpenFoam-based computational fluid dynamics analysis," Phys. Fluids **34**, 013318 (2022).
[11]M. R. Pendar and J. C. Páscoa, "Numerical modeling of the distribution of virus carrying saliva droplets during sneeze and cough," Phys. Fluids **32**, 083305 (2020).
[12]V. Vuorinen, M. Aarnio, M. Alava, V. Alopaeus, N. Atanasova, M. Auvinen, N. Balasubramanian, H. Bordbar, P. Erästö, R. Grande, N. Hayward, A. Hellsten, S. Hostikka, J. Hokkanen, O. Kaario, A. Karvinen, I. Kivistö, M. Korhonen, R. Kosonen, J. Kuusela, S. Lestinen, E. Laurila, H. J. Nieminen, P. Peltonen, J. Pokki, A. Puisto, P. Råback, H. Salmenjoki, T. Sironen, and M. Österberg, "Modelling aerosol transport and virus exposure with numerical simulations in relation to SARS-CoV-2 transmission by inhalation indoors," Saf. Sci. **130**, 104866 (2020).
[13]M. Auvinen, J. Kuula, T. Grönholm, M. Sühring, and A. Hellsten, "High-resolution large-eddy simulation of indoor turbulence and its effect on airborne transmission of respiratory pathogens—Model validation and infection probability analysis," Phys. Fluids **34**, 015124 (2022).
[14]H. Calmet, K. Inthavong, A. Both, A. Surapaneni, D. Mira, B. Egukitza, and G. Houzeaux, "Large eddy simulation of cough jet dynamics, droplet transport, and inhalability over a ten minute exposure," Phys. Fluids **33**, 125122 (2021).
[15]J. M. Cepress, J. F. Cummings, C. D. Ricketts, J. W. Clymer, and G. A. Tommaselli, "Comparison of trocar performance in consideration of the COVID-19 pandemic," Med. Devices Diagn. Eng. **5**, 1–7 (2020).
[16]N. G. Mowbray, J. Ansell, J. Horwood, J. Cornish, P. Rizkallah, A. Parker, P. Wall, A. Spinelli, and J. Torkington, "Safe management of surgical smoke in the age of COVID-19," Br. J. Surg. **107**, 1406–1413 (2020).
[17]F. Ducros, F. Nicoud, and T. Poinsot, "Wall-adapting local eddy-viscosity models for simulations in complex geometries," in *Numerical Methods for Fluid Dynamics VI* (ICFD, 1998), pp. 293–299.
[18]F. Akagi, I. Haraga, S. I. Inage, and K. Akiyoshi, "Effect of sneezing on the flow around a face shield," Phys. Fluids **32**, 127105 (2020).
[19]W. H. Finlay, "Motion of a single aerosol particle in a fluid," in *The Mechanics of Inhaled Pharmaceutical Aerosols* (Academic Press, 2001), pp. 17–45.
[20]F. Coccolini, D. Tartaglia, A. Puglisi, C. Giordano, M. Pistello, M. Lodato, and M. Chiarugi, "SARS-CoV-2 is present in peritoneal fluid in COVID-19 patients," Ann. Surg. **272**, E240–E242 (2020).
[21]I. Cheruiyot, P. Sehmi, B. Ngure, M. Misiani, P. Karau, B. Olabu, B. M. Henry, G. Lippi, R. Cirocchi, and J. Ogeng'o, "Laparoscopic surgery during the COVID-19 pandemic: Detection of SARS-COV-2 in abdominal tissues, fluids, and surgical smoke," Langenbeck's Arch. Surg. **406**, 1007–1014 (2021).
[22]R. Mallick, F. Odejinmi, and T. J. Clarke, "COVID-19 pandemic and gynaecological laparoscopic surgery: Knowns and unknowns," Facts, Views Vis Obgyn **12**, 3–7 (2020).
[23]L. Stotz, R. Joukhadar, A. Hamza, F. Thangarajah, D. Bardens, I. Juhasz-Böss, E. F. Solomayer, M. P. Radosa, and J. C. Radosa, "Instrument usage in laparoscopic gynecologic surgery: A prospective clinical trial," Arch. Gynecol. Obstet. **298**, 773–779 (2018).
[24]L. Bourouiba, E. Dehandschoewercker, and J. W. M. Bush, "Violent expiratory events: On coughing and sneezing," J. Fluid Mech. **745**, 537–563 (2014).
[25]S. Verma, M. Dhanak, and J. Frankenfield, "Visualizing the effectiveness of face masks in obstructing respiratory jets," Phys. Fluids **32**, 061708 (2020).
[26]X. Xie, Y. Li, A. T. Y. Chwang, P. L. Ho, and W. H. Seto, "How far droplets can move in indoor environments–revisiting the Wells evaporation-falling curve," Indoor air **17**, 211–225 (2007).
[27]D. K. Milton, M. P. Fabian, B. J. Cowling, M. L. Grantham, and J. J. McDevitt, "Influenza virus aerosols in human exhaled breath: Particle size, culturability, and effect of surgical masks," PLoS Pathog. **9**, e1003205 (2013).
[28]L. Schultz, "An analysis of surgical smoke plume components, capture, and evacuation," AORN J. **99**, 289–298 (2014).

[29]A. Tcharkhtchi, N. Abbasnezhad, M. Zarbini Seydani, N. Zirak, S. Farzaneh, and M. Shirinbayan, "An overview of filtration efficiency through the masks: Mechanisms of the aerosols penetration," Bioactive Mater. **6**, 106–122 (2021).
[30]J. M. Uecker, A. Fagerberg, N. Ahmad, A. Cohen, M. Gilkey, F. Alembeigi, and C. R. Idelson, "Stop the leak!: Mitigating potential exposure of aerosolized COVID-19 during laparoscopic surgery," Surg. Endosc. **35**, 493–501 (2021).
[31]L. Nicolaou and T. Zaki, "Characterization of aerosol stokes number in 90° bends and idealized extrathoracic airways," J. Aerosol Sci. **102**, 105–127 (2016).
[32]P. Demokritou, S. J. Lee, S. T. Ferguson, and P. Koutrakis, "A compact multi-stage (cascade) impactor for the characterization of atmospheric aerosols," J. Aerosol Sci. **35**, 281–299 (2004).